Conditional Depletion of Hippocampal Brain-Derived Neurotrophic Factor Exacerbates Neuropathology in a Mouse Model of Alzheimer's Disease

David J. Braun[1], Sergey Kalinin[1], and Douglas L. Feinstein[2]

Abstract

Damage occurring to noradrenergic neurons in the locus coeruleus (LC) contributes to the evolution of neuroinflammation and neurodegeneration in a variety of conditions and diseases. One cause of LC damage may be loss of neurotrophic support from LC target regions. We tested this hypothesis by conditional unilateral knockout of brain-derived neurotrophic factor (BDNF) in adult mice. To evaluate the consequences of BDNF loss in the context of neurodegeneration, the mice harbored familial mutations for human amyloid precursor protein and presenilin-1. In these mice, BDNF depletion reduced tyrosine hydroxylase staining, a marker of noradrenergic neurons, in the rostral LC. BDNF depletion also reduced noradrenergic innervation in the hippocampus, the frontal cortex, and molecular layer of the cerebellum, assessed by staining for dopamine beta hydroxylase. BDNF depletion led to an increase in cortical amyloid plaque numbers and size but was without effect on plaque numbers in the striatum, a site with minimal innervation from the LC. Interestingly, cortical Iba1 staining for microglia was reduced by BDNF depletion and was correlated with reduced dopamine beta hydroxylase staining. These data demonstrate that reduction of BDNF levels in an LC target region can cause retrograde damage to LC neurons, leading to exacerbation of neuropathology in distinct LC target areas. Methods to reduce BDNF loss or supplement BDNF levels may be of value to reduce neurodegenerative processes normally limited by LC noradrenergic activities.

Introduction

It has been well known for almost 50 years that noradrenergic (NAergic) neurons located in the brainstem area known as the locus coeruleus (LC) are damaged or lost in Alzheimer's disease (AD). LC neuronal loss of about 25% occurs naturally during aging and is associated with reductions in central nervous system (CNS) noradrenaline (NA) levels of about 50% in certain brain regions (reviewed in Mann, 1983). Although LC neuronal damage is present in other neurodegenerative diseases, the extent of cell loss in AD has been estimated at up to about 70% and is among the highest (Chris et al., 2003). The LC plays important roles in the regulation of behaviors such as anxiety, depression, and attention (Szabadi, 2013). However, the consequences of LC neuronal loss within the context of neuropathology are not fully known. Experimental manipulation in animal models of AD show that LC neuronal loss leads to an exacerbation of AD-type pathology (Kalinin et al., 2007; Heneka et al., 2010) suggesting a role in limiting disease

[1]Department of Anesthesiology, University of Illinois, Chicago, IL, USA
[2]Jesse Brown VA Medical Center, Chicago, IL, USA

Corresponding Author:
Douglas L. Feinstein, 835 South Wolcott Street, MC 513, Room E720, Chicago, IL 60612, USA.
Email: dlfeins@uic.edu

progression. Consistent with this role, numerous studies in mouse models of AD have shown that interventions which reduce LC damage or restore NA levels can reduce various indices of AD pathology including that of glial cell activation, amyloid burden, and cognitive deficits (Kalinin et al., 2012; Braun et al., 2014). Taken together, these findings indicate that methods to reduce LC damage or enhance NA-signaling pathways should provide benefit in AD and related conditions. While clinical trials to directly test this hypothesis have not yet been carried out, observations that use of adrenoceptor modulators can reduce noncognitive deficits in AD patients (Peskind et al., 2005; Wang et al., 2009), and that genetic polymorphisms in NA-relevant genes are associated with AD risk (Yu et al., 2008; Combarros et al., 2010) are consistent with this possibility.

To develop means to reduce LC damage, a knowledge of factors responsible is required. In this regard, the causes of LC damage are not well known, but LC neurons are speculated to be particularly vulnerable to insult due to a combination of high bioenergetic need (Sanchez-Padilla et al., 2014), high-oxidative stress as a byproduct of NA synthesis (Tekin et al., 2014), large exposure to blood circulation (Pamphlett, 2014), and sensitivity to both central and peripheral inflammation (Kaneko et al., 2005; Hopp et al., 2015). Of interest, one putative cause of LC damage is a loss of neurotrophic support from areas to which LC neurons project. Among the factors with an established role in LC survival is brain-derived neurotrophic factor (BDNF). It has been shown that the phenotypic differentiation of LC neurons requires BDNF (Sabine et al., 2006), and that LC neuronal number is reduced in mice that lack BDNF (Luellen et al., 2007) or the BDNF receptor TrkB (Holm et al., 2003). In addition, experiments utilizing infusion of BDNF into the cortex (CTX) induces significant sprouting of NAergic axon terminals, while infusion of anti-BDNF results in the opposite (Nakai et al., 2006). Interestingly, these effects were observed only in aged 19-month-old and not younger 13-month-old rats, suggesting that BDNF functions to maintain NAergic connections specifically in the context of aging. It has been reported that CNS NA levels and NAergic projections are increased with aging (Raskind et al., 1999; Matsunaga et al., 2004; Matsunaga et al., 2006) despite a decline in LC cell number (Manaye et al., 1995). Thus, BDNF may be required to maintain these compensatory increases in NAergic innervation.

The above studies demonstrate that BDNF can influence parameters of NAergic innervation, suggesting that loss of BDNF in LC projection areas will adversely affect NAergic signaling. In support of this, the LC strongly innervates the CTX and hippocampus (HC), where BDNF levels are substantially decreased in AD

(Connor et al., 1997). In addition, postmortem observations of AD show that degeneration occurs preferentially in the rostral and central portion of the LC, areas with neurons projecting to HC and CTX (Marcyniuk et al., 1986). Further support comes from studies in aged AD model mice, where LC neuronal atrophy, an indicator of cellular stress, is restricted to regions projecting to HC and CTX (German et al., 2005). Whether targeted disruption of BDNF in LC projection areas leads to LC damage has not been directly tested.

The causes of BDNF loss are also not well known; however, the fact that NA signaling increases BDNF expression (Chen et al., 2007; Jurič et al., 2008, and that drugs which increase NA increase BDNF expression *in vivo* (Kalinin et al., 2012), raises the possibility of a feedback loop for LC damage: Declining neurotrophic support exacerbates LC stress and NAergic dysfunction, which in turn exacerbates target field BDNF depletion, resulting ultimately in substantial LC damage and NAergic denervation. To address this possibility, we have examined the consequences of targeted depletion of HC BDNF on LC damage within the context of AD pathology. Our results show that loss of BDNF from one LC target region reduces NA biosynthetic enzymes both within the LC as well as other terminal fields and also leads to increased indices of AD-type pathology (inflammation, amyloid burden) in distinct LC-target areas. Together these findings provide a mechanism that can help account for dissemination of pathology throughout the CNS.

Methods and Materials

Materials

All general laboratory reagents were obtained from Sigma Chemical Company (St. Louis, MO, USA).

Animals

The BDNF[TM3JAE] mouse line was obtained from JAX Mice (Jackson Laboratory, Bar Harbor, ME, USA). These mice (referred herein as BDNF[f/f]) contain a BDNF transgene with the protein-coding exon V flanked by loxP sites, originally generated by Jaenisch and coworkers (Rios et al., 2001). The BDNF[f/f] mice were originally derived from strain 129S4/SvJae, inbred over 15 generations, then bred for 2 generations into C56BL/6 mice (Charles River, Wilmington, MA, USA). The 5XFAD mice (Ohno et al., 2004) express 3 mutations in the amyloid precursor protein (APP) and 2 mutation in presenilin-1 (PS1) and have been maintained for over 10 generations on a C57BL/6 background. BDNF[f/f] mice were crossed with 5XFAD mice to generate pups
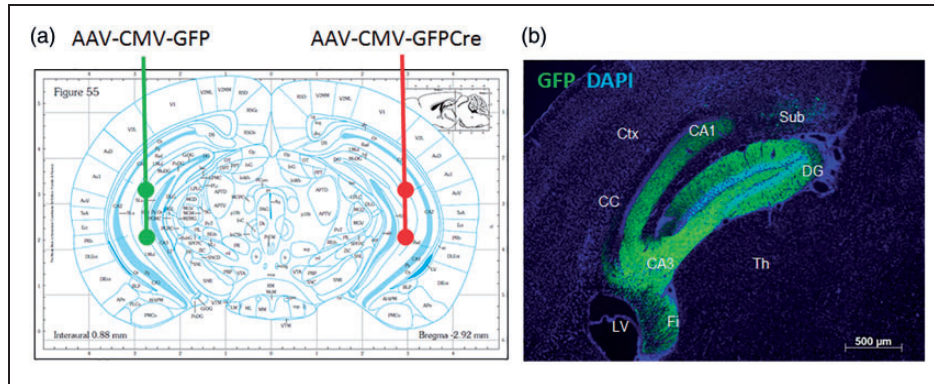
Figure 1. Experimental design of brain-derived neurotrophic factor depletion.
(a) WT (BDNF$^{f/f}$: 5XFAD$^{-/-}$) and 5XFAD (BDNF$^{f/f}$: 5xFAD$^{+/-}$) mice were injected in the CA1 and CA3 regions (Bregma coordinates −2.9 mm A/P, ± 2.8 mm M/L, −2.5 and −4.0 mm D/V) of the HC with two 1-µL injections of 1 × 10^9 GC/µL AAV9-CMV-GFP virus into the left HC, and two 1-µL injections of 1 × 10^9 GC/µL AAV9-CMV-GFP-Cre virus into the right HC. (b) Representative section showing GFP fluorescence localized to the HC at 4 weeks after injection into a BDNF$^{f/f}$: 5XFAD$^{-/-}$ mouse with AAV-CMV-GFP.
Ctx = cortex; LV = lateral ventricle; Th = thalamus; Sub = subiculum; Fi = fimbria of the hippocampus; CC = corpus callosum; DG = dentate gyrus.

heterozygous for both the BDNF floxed allele and the 5XFAD transgenes. These mice were then backcrossed with homozygous BDNF$^{f/f}$ mice to generate ~25% 5XFAD (5XFAD$^{+/-}$): BDNF$^{f/f}$ mice. Genotyping was performed when mice were 3 weeks of age using purified genomic DNA isolated from tail, with recommended protocols (Jackson Laboratory, Bar Harbor, ME, USA). All animals were housed 3 to 5 animals per cage, fed *ad libitum*, and maintained on a 12:12 hr light dark cycle. Mice were aged 7 to 7.5 months at time of surgery and allowed to survive for another 4 weeks before sacrifice and brain tissue analysis.

Viruses

Adeno-associated viruses, serotype 9 (AAV9), were obtained from Penn Vector Core at the Perelman School of Medicine at the University of Pennsylvania. For knockout (KO) studies, AAV9.CMV.HI.eGFP-Cre.WPRE.SV40 (AAV-Cre), directing expression of bacterial Cre recombinase (catalag # AV-9-PV2004) attached to the fluorescent reporter molecule enhanced green fluorescent protein (eGFP) was chosen for its broad tropism, ability to diffuse into a relatively large area, and low-inflammatory induction (Karra and Dahm, 2010; Aschauer et al., 2013). The cytomegalovirus (CMV) promoter was chosen since it is expressed in a variety of cell types. For control injections, AAV9.CMV.PI.eGFP.WPRE.bGH (catalog #AV-9-PV0101) directing expression of the same eGFP (AAV-GFP) was used. Immediately before use, viruses were diluted 1:10 in sterile phosphate buffered saline (PBS), for a final titer of approximately 1 × 10^9 genocopies per µL.

Stereotactic Injection of AAV

5XFAD:BDNF$^{f/f}$ mice were aged 7 to 7.5 months at time of injection. Animals received unilateral injections of either AAV-GFP or AAV-Cre. Animals were injected with AAV-GFP into the left HC and AAV-Cre into the right HC (Figure 1(a)). Animals were anesthetized with intraperitoneal injections of 100/10 mg/kg ketamine/xylazine and given 0.1 mg/kg buprenorphine subcutaneously for pain management. Depth of anesthesia was assessed via toe-pinch. The mice had their heads shaved and restrained in a stereotaxic frame with mouse adapter (Stoeltling, Wood Dale, IL). Sterile Bausch & Lomb erythromycin ophthalmic ointment (0.5%) was applied to the eyes to keep them from drying out, and their heads cleaned with 70% ethanol. A small incision was made in the skin down the midline of the cranium, exposing the skull landmarks lambda and Bregma. Hydrogen peroxide was used to clean the top of the skull. Target injection coordinates were mapped from Bregma, and a small hole drilled through the skull directly above target sites with a bone drill. Each HC of each animal received two 1-µL injections, into areas CA1 and CA3. CA1 coordinates were −2.9 mm A/P, ± 2.8 mm M/L, and −2.5 mm D/V. CA3 coordinates were the same, except the D/V depth was −4 mm. Injection rate was 0.2 µL per minute, for a total of 5 min per injection, and the needle left in place for 1-min postinjection. After injections, the incision was sutured and Neosporin applied. Animals recovered on heating pads until awake and monitored 1, 2, 7, and 10 days postsurgery. All surgeries were performed with IACUC approval. The animals were allowed to survive for 4 weeks postinjection to allow viral

expression and BDNF depletion, then sacrificed for histological processing of brain tissue.

Tissue Collection

Four weeks after viral injection, animals were asphyxiated with carbon dioxide in a rodent euthanasia chamber and transcardially perfused with PBS, followed by 4% paraformaldehyde. Brains were removed and postfixed in 4% paraformaldehyde for 48 hr, followed by 2 days in 30% sucrose solution for cryoprotection. Samples were then cut down the midline, and each hemisphere embedded separately in Tissue-Tek optimum cutting temperature compound, rapidly frozen in isopentane cooled to $-55°C$, and stored at $-80°C$ until ready for sectioning.

Histo- and Immunohistochemistry

Frozen sections were cut to 25 μm. Sections were placed in freezing solution (PBS, 40% ethylene glycol, 30% glycerol) at $-20°C$ until ready for subsequent staining. Prior to staining, sections were washed $3\times$ in PBS for 5 min each. Sections were incubated in blocking solution (PBS with 0.1% Triton X-100 and 5% normal donkey serum) for 1 hr. Primary antibodies used were rabbit polyclonal against BDNF (catalog # sc-546, Santa Cruz Biotechnology, Dallas, TX, USA; 1:250 dilution), rabbit polyclonal against tyrosine hydroxylase (TH; catalog # P40101-150, PelFreez, Rogers, AR, USA; 1:1000 dilution), goat polyclonal against dopamine beta hydroxylase (DβH; catalog # sc-7486, Santa Cruz Biotechnology, Dallas, TX, USA; 1:250 dilution), rabbit polyclonal against Iba1 (Wako, Richmond, VA, USA; 1:1000 dilution), and rat monoclonal against Glial fibrillary acidic protein (GFAP; B2.210, Trojanowski et al., 1986, 1:1000 dilution). Sections were incubated overnight at 4°C in primary antibody, washed $3\times$ in PBS for 5 min each, and then incubated in Rhodamine Red-X or fluorescein-conjugated secondary antibodies (Vector Laboratories, Burlingame, CA, USA) diluted 1:100 in blocking solution. Negative control sections were prepared in identical manner but without the primary antibody. Sections were counterstained with 4′,6-diamidino-2-phenylindole (DAPI) and either mounted with Vectashield® H-1000 mounting medium (Vector labs) or subsequently stained with Thioflavin S (ThioS). ThioS staining was done by placing sections in filtered ThioS solution (1% ThioS in distilled water) for 5 min on a shaker, light protected. They were then washed $2\times$ in 80% ethanol for 5 min each and coverslipped with Vectashield H-1000 as earlier. Sections stained for DβH underwent primary staining as earlier but with biotin-conjugated secondary antibody for 1 hr, followed by another hour with streptavidin-conjugated Alexa Fluor® 568. The DβH sections were subsequently stained with ThioS.

Image Acquisition and Analysis

TH staining intensity was quantified in three sections per mouse from three different mice, the sections contained both the rostral and caudal portions of the LC. Matched sections (one set derived from the left AAV-GFP injected side, the other set from right AAV-Cre injected side) were obtained from the same mice, aligned by the sectioning distance from midline, and refined by blinded side-by-side anatomical comparisons, including by matching ventricle size and shape, and morphology of the HC within the section. The sections were collected consecutively, and every sixth to seventh section was used for staining with the same antibody. DβH was quantified as the number of puncta in three different regions, the HC, the cerebral CTX, and the cerebellum (CB). Quantitation in the HC was done in the CA1, CA3, and dentate gyrus (DG) areas. Quantitation in the CTX encompassed primarily the frontal association CTX. Quantitation in the CB was done in the molecular layer of the ansiform lobule. GFAP and Iba1 were quantified as the number of positive-staining cells in the CTX. The number of ThioS positively stained plaques were quantified in the CTX and striatum. For DβH, ThioS, GFAP, and Iba1, staining was quantified in four different mice, in a total of 8 to 12 sections per side per animal. All imaging was performed with a Zeiss Axioplan 2 epifluorescent microscope, with attached AxioCam MRm camera. Axiovision software version 4.7 was used for image acquisition and quantification.

Images for GFAP, Iba1, and DβH staining were collected with a $40\times$ objective, providing a total field of view of 0.16 mm^2 of which .09 mm^2 was captured by the camera. Images for ThioS staining were collected with a $20\times$ objective, providing a field of view of 0.64 mm^2, of which 0.36 mm^2 was captured by the camera. One field of view from each section was quantified; those were selected to be in the same area of the CTX, HC, and CB in each of the different sections. Axiovision software parameters were set to define positive staining versus background threshold values, obtained from the same regions in negative control sections (lacking the primary antibody). For GFAP, Iba1, and TH staining, a cutoff value of $>20 \mu m^2$ was used to identify cells. For counting of ThioS and DβH puncate staining, all objects with staining over background values were counted. Slides were examined in a blinded manner.

Statistical Analyses and Data Presentation

All statistical analyses were performed using GraphPad Prism version 7.0. Ratio paired nonparametric T tests were used to compare brain regions in treatment- and control-matched hemispheres. Correlational analyses were carried out by nonparametric Spearman analyses.

Where mean values are reported in the text, the standard deviation (*SD*) is reported following the mean.

Results

Targeted Depletion of Hippocampal BDNF

We used stereotactic microinjection to deliver virally encoded Cre recombinase into BDNF$^{f/f}$ mice to allow localized depletion from the HC in multiple cellular sources. Examination of GFP fluorescence showed good coverage of the virus within the HC. GFP was visible throughout the structure, encompassing the CA1, CA3, and DG areas, as well as the subiculum and fimbria (Figure 1(b)). Light staining was observed in the cortical area dorsal to the CA1 region. GFP staining was low or undetectable outside of these regions. Immunostaining of sections from AAV-GFP and AAV-Cre injected mice showed reduced BDNF staining in and around the HC on the AAV-Cre injected side (Figure 2).

Hippocampal BDNF Depletion Reduces LC TH Expression

The consequences of HC BDNF depletion on the LC in 5XFAD mice were first examined by staining for TH, the rate limiting step in NA synthesis, which is expressed in all mature LC NAergic neurons. Sections containing the LC from the hemisphere of BDNF$^{f/f}$: 5XFAD$^{+/−}$ mice injected with AAV-Cre (BDNF KO sections) were compared with matched sections from the contralateral LC (control sections; Figure 3). Immunostaining for TH showed reduced staining in the rostral LC (Figure 3(a)) but not in the caudal portion of the LC (Figure 3(b)). Quantitative analysis confirmed the rostral LC had a statistically significant decline (27%) of average intensity of TH staining in BDNF KO sections compared with

controls (Figure 3(c)), while a smaller decrease (roughly 25%) in the caudal LC did not reach statistical significance (Figure 3(d)).

Effect of Hippocampal BDNF Depletion on NAergic Innervation

Reduced LC TH expression could reduce NAergic innervation to target areas. To test this, sagittal sections from control and BDNF KO hemispheres from 5XFAD mice were stained for DβH, a marker of NAergic projections (Figure 4). Quantitative analysis showed that the total DβH staining combined from the CA1, CA3, and DG hippocampal regions was significantly reduced (from 505 ± 226 to 308 ± 158 puncta, control and BDNF KO, respectively; Figure 4(d)). Analysis of individual HC subregions revealed a trend toward reduced puncta in the CA1 region ($p = .057$, paired *t* test; Figure 4(e)) and lesser changes in the CA3 and DG regions. Interestingly, DβH puncta were also reduced by BDNF depletion in the CB (decreasing from 2023 ± 450 to 1188 ± 356 puncta; Figure 5(a) and (b)) and frontal CTX (decreasing from 224 ± 125 to 99 ± 27, $p = .051$, paired *t* test; Figure 5(c) and (d)). In contrast to the 5XFAD mice, BDNF depletion did not decrease DβH staining relative to the control sections in wild type (WT) mice, either in the HC (Figure 6(a) and (b)) or in the CB (Figure 6(c)). Comparison of total DβH staining shows a significant increase in the 5XFAD compared with WT mice (Figure 6(d)).

Effect of Hippocampal BDNF Depletion on Amyloid Plaque Load

Reduced NAergic innervation and consequent reduced NA release could exacerbate AD-type pathology in the 5XFAD mice. To test this, amyloid plaque burden was
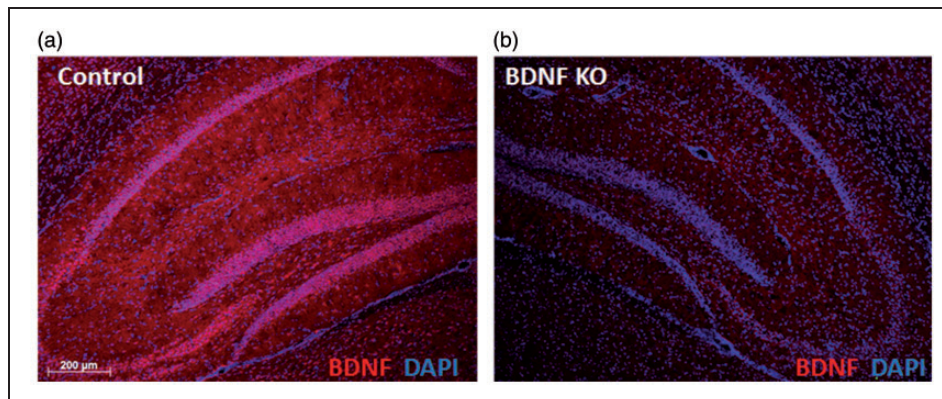
Figure 2. Four-week viral expression depletes hippocampus brain-derived neurotrophic factor.
Representative images of BDNF staining in the HC from (a) AAV-GFP injected (control) and (b) AAV-Cre injected (BDNF KO) BDNF$^{f/f}$: 5XFAD$^{−/−}$ mice.
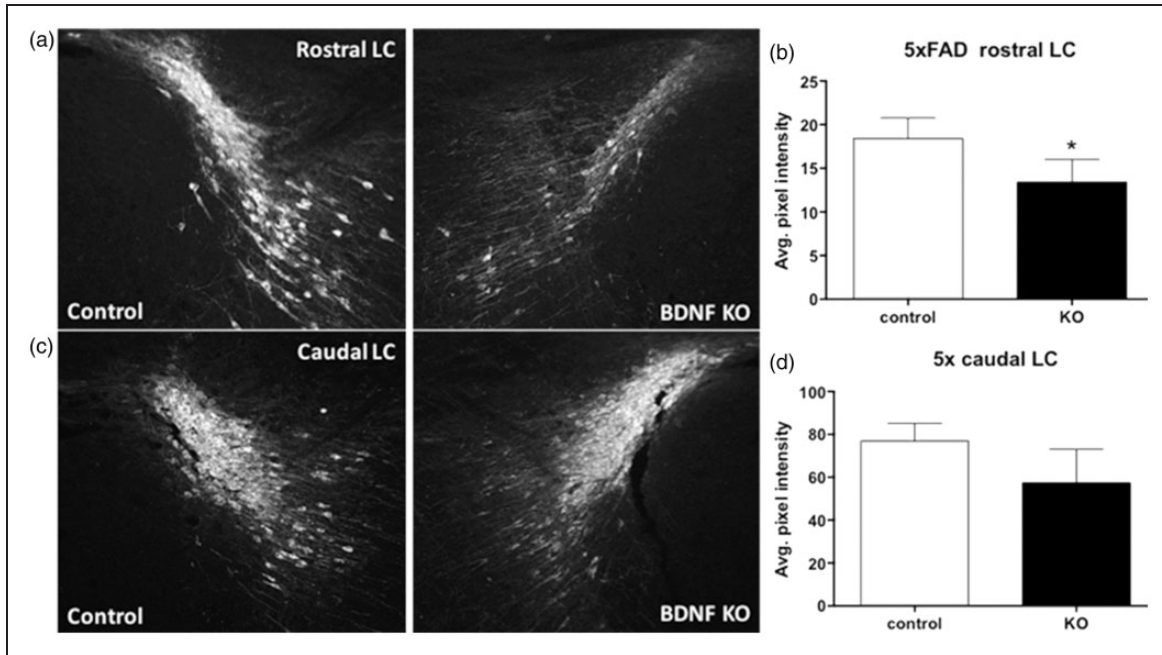
Figure 3. Hippocampus brain-derived neurotrophic factor depletion reduces tyrosine hydroxylase staining in the rostral LC. Representative images of TH staining in the (a) rostral and (c) caudal aspects of the LC of BDNF[f/f]: 5XFAD^{+/−} mice injected with AAV-Cre on one side (BDNF KO), and AAV-GFP on the contralateral side (control). (b) and (d) Quantitation of TH staining intensity shows a decrease in the (b) rostral LC ipsilateral to the site of BDNF depletion. Data are mean $\pm$ SEM, $n = 3$ matched pairs, three sections per ipsilateral, and three sections per contralateral LC.
*$p < .05$, Students paired t test.

assessed by ThioS staining for dense core plaques. The frontal CTX was chosen as an area that has substantial NAergic innervation from the LC as well as significant plaque pathology in 5XFAD mice. In the CTX, the average number of plaques per field of view increased from a mean of 15.3 ± 3.4 in control to 22.3 ± 6.6 (Figure 7(b)) in BDNF KO hemispheres; and the average plaque size increased from 30.2 ± 2.6 to $38.4 \pm 3.3\,\mu m^2$ (Figure 7(c)). In contrast, in the striatum, which does not receive NAergic innervation from the LC, there was no significant difference in plaque number between control and BDNF KO hemispheres (Figure 7(d)). These data support an indirect effect of HC BDNF depletion on cortical plaque pathology, mediated via damage to the LC.

Hippocampal BDNF Depletion Alters Microglial Activation

Both astrocytes and microglia influence plaque clearance and respond to NA, suggesting that increased plaque load could be due to reductions of LC signaling to glial cells which can reduce amyloid levels via phagocytosis or production of proteases involved in amyloid degradation. To test this, CTX sections were stained for GFAP to label astrocytes (Figure 8(a) and (b)) and Iba1 to label microglia (Figure 8(c) and (d)). While there was no significant effect of BDNF depletion on the number of GFAP+

stained astrocytes, we observed a significant decrease in the number of Iba1+ stained microglial cells (decreasing from 1148 ± 466 to 583 ± 158). Comparison of the number of Iba1+ cells to the number of DβH puncta in the CTX, using data from both the control and the BDNF KO sections (Figure 8(e)), shows a strong positive correlation, suggesting that microglia cell numbers or activation state (regardless of BDNF content) is dependent upon NAergic innervation.

Discussion

Results from this study show that depletion of BDNF from a target site of LC innervation leads to damage to NAergic neurons within the LC, as well as to secondary consequences in distinct LC target regions (CTX, CB), including significant reductions in NAergic innervation, increases in amyloid burden, and a reduced number of Iba1 positively stained microglial cells. As illustrated in Figure 9, the causes of HC BDNF loss may be experimental as in the current study, or due to other factors such as environmental toxins, other genetic variations, or to the disease process itself. The loss of neurotrophic support to the LC results in reduced NAergic signaling, which ultimately influences glial functions throughout the CNS. At 4 weeks after viral delivery, immunostaining for BDNF in the HC showed a large reduction in staining
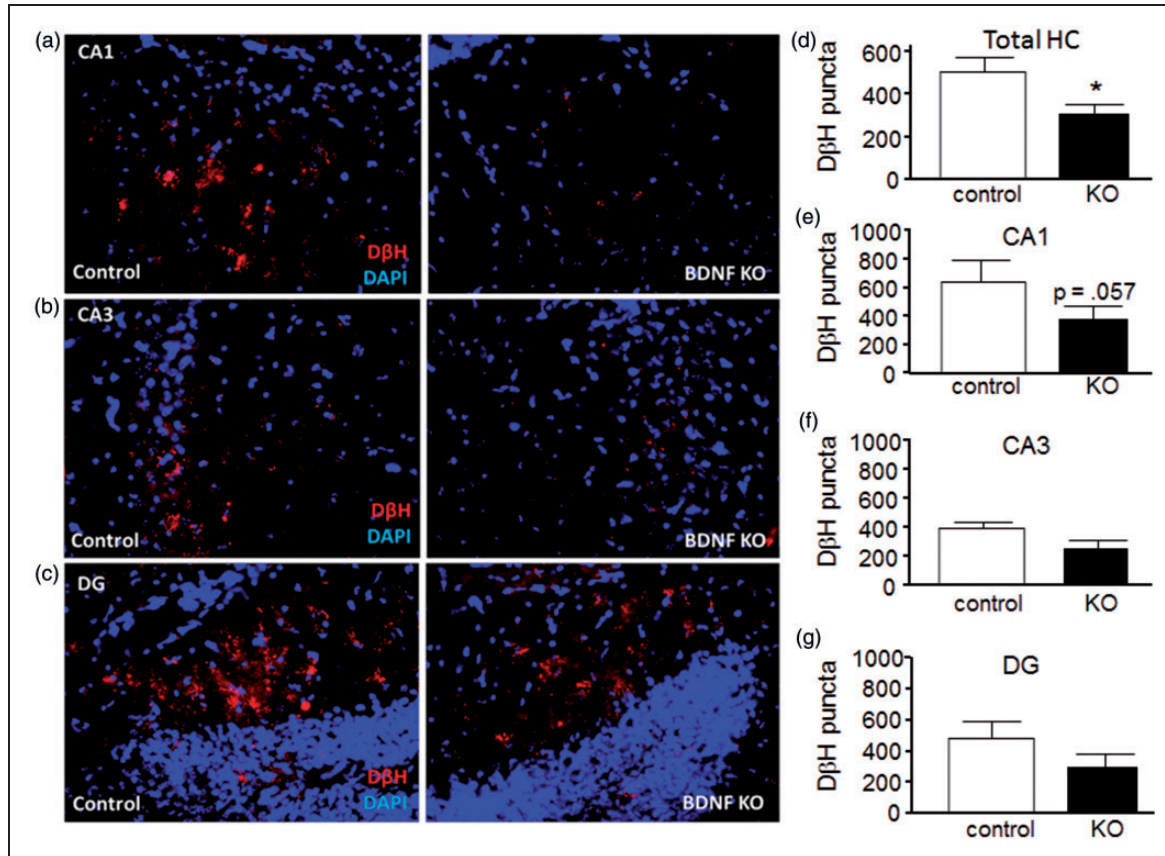
Figure 4. Effect of hippocampus brain-derived neurotrophic factor depletion on noradrenergic innervation in hippocampus. Representative images of HC areas CA1 (a), CA3 (b), and DG (c) from AAV-GFP injected (left, control) and AAV-Cre injected (right, BDNF KO) sides of BDNF$^{f/f}$: 5XFAD$^{+/-}$ mice. (d) to (g) Quantitation shows a significant reduction in total DβH (combined staining from the three regions) on the BDNF KO side (d), while in the individual subregions BDNF depletion caused an almost-significant reduction in DβH staining in CA1 (e), and nonsignificant reductions in areas CA3 (f) and DG (g). Data are mean $\pm$ *SEM*, $n = 4$ matched pairs, 8 to 12 sections per side per animal.
*$p < .05$, Student's paired *t* test.

in both cellular elements as well within the intercellular spaces, consistent with reduced BDNF expression and export. Although we did not carry out a quantitative analysis of BDNF protein depletion (due to limited numbers of sections available), there is substantial evidence that microinjection of AAV virus expressing Cre recombinase under control of a CMV promoter will efficiently lead to excision of floxed genes. The BDNF$^{f/f}$ mice used in the current study (Bdnf ^{tm3Jae}) have been used by others and shown that the BDNF floxed exon is efficiently excised in the presence of Cre recombinase. The mice were originally used to cross to a CamK2a-Cre mouse which deleted BDNF throughout the brain from birth (Rios et al., 2001) and assessed for changes in various indices of anxiety. In that study, excision of the floxed BDNF allele was confirmed by northern blot analysis showing reductions in BDNF mRNA in different brain regions. The same mice were used to examine the effects

of HC BDNF deletion on learning and fear responses, accomplished by microinjection of a lentivirus expressing Cre recombinase under control of the CMV promoter into the HC (Heldt et al., 2007), and excision was confirmed by in situ hybridization for BDNF mRNA. Microinjection of other virally expressed Cre recombinases into the HC has been done numerous times, demonstrating that this method can efficiently induce excision of floxed genes. One of the first reports of using this method was stereotactic injection of an AAV-CMV-Cre into the HC to activate b-galactosidase expression in Rosa26 reporter mice (Kaspar et al., 2002; Ahmed et al., 2004), without appearance of any obvious toxic effects. Those studies also showed that the AAV vector infects both neurons and glial cells, although neurons were more strongly labeled. Similarly, AAV-CMV-Cre delivery via microinjection into the HC has been used to delete target genes including the leptin receptor B which was
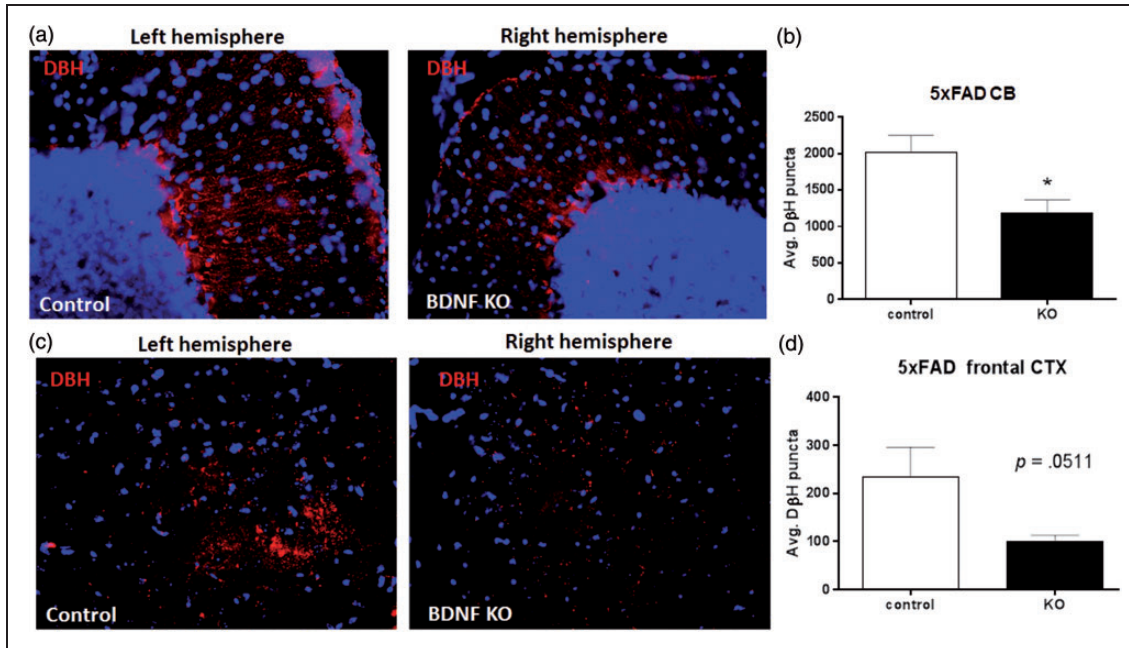
Figure 5. Hippocampus brain-derived neurotrophic factor depletion reduces noradrenergic innervation in cerebellum and cortex.
(a) Representative images of CB contralateral (left, control) and ipsilateral (right, BDNF KO) to site of BDNF depletion in BDNF$^{f/f}$:
5XFAD$^{+/-}$ mice. (b) Quantitation shows a significant decline in DβH puncta in the BDNF KO CB compared with the control CB. (c)
Representative images of frontal CTX contralateral (left, control) and ipsilateral (right, BDNF KO) to site of BDNF depletion in BDNF$^{f/f}$:
5XFAD$^{+/-}$ mice. (d) Quantitation shows an almost significant decline in DβH puncta in the BDNF KO versus the control CTX. Data show
mean $\pm$ SEM, $n = 4$ matched pairs, 8 to 12 sections per side per animal.
Student's t test, $*p < .05$.

confirmed by reverse transcription polymerase chain reaction analysis of hippocampal mRNA for the deleted exon (Guo et al., 2013); and for the A2AR which was confirmed by polymerase chain reactionas well as receptor binding (Wei et al., 2014). Based on these findings, others have used similar methods and relied upon either the presence of AAV-encoded GFP fluorescence or of the appearance of downstream events as evidence of gene deletion. Injection of AAV-CAG-T2A driven Cre recombinase into the HC to delete the PTEN gene led to reduced immunostaining for downstream targets of PTEN (Yang et al., 2015), injection of a lentiviral CMV-Cre recombinase to delete HC neuroligin blocked long-term potentiation (Jiang et al., 2010), and injection of AAV-CMV-Cre-GFP into the HC to delete the ATR (ataxia telangiectasia-mutated and rad-3-related protein) gene led to appearance of GFP fluorescence in the HC as well as alterations in behavior (Onksen et al., 2012). Together with our observations of alterations in LC TH staining, amyloid plaque numbers, and microglial Iba1 staining in the AAV-CMV-Cre versus the AAV-CMV-GFP injected hemispheres, we conclude that Cre-mediated BDNF depletion accounts for the changes observed.

Reduced TH staining was observed in the rostral, with smaller reductions observed in the caudal area of the LC.

This may be expected since NAergic neurons in the rostral LC project primarily to the HC. The loss of TH staining suggests that LC neurons are damaged by lack of BDNF support; consistent with this we observed that the number LC NAergic projections were also reduced in the BDNF KO hemispheres compared with control hemisphere. However, the loss of NAergic innervation was observed in 5XFAD:BDNF$^{f/f}$ mice but not WT mice. This suggests that in WT mice, BDNF is not a major factor in maintaining NAergic innervation, or that compensatory mechanisms exist in WT mice that are able to rescue the effect of BDNF loss. These data also suggest that 5XFAD mice are more susceptible to hippocampal BDNF depletion than WT littermates and indicate that loss of NAergic innervation occurs in multiple areas innervated by the LC, consistent with the presence of damage throughout the LC nucleus.

We also observed that NAergic innervation in the 5XFAD:BDNF$^{f/f}$ mice was significantly greater than that in the WT mice, suggesting that AD-type pathology in the 5XFAD mice leads to a compensatory increase in innervation. These results are consistent with a previous study (Matsunaga et al., 2004) where BDNF depletion only affected innervation in aged animals who had increased innervation and suggests that BDNF plays a role in maintaining the enhancement of NAergic
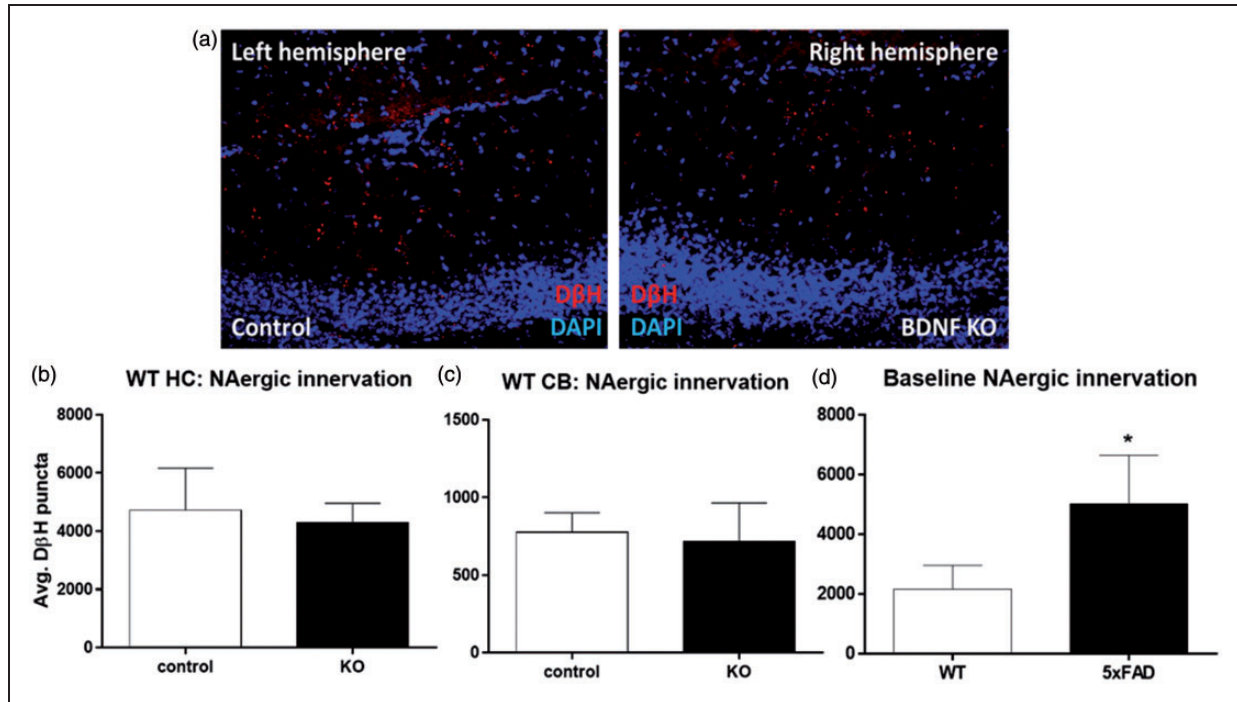
Figure 6. Hippocampus brain-derived neurotrophic factor depletion does not alter noradrenergic innervation in wild type mice. (a) Representative images of AAV-GFP injected (left, control) and AAV-Cre injected (right, BDNF KO) HC from a WT (BDNF$^{f/f}$: 5XFAD$^{-/-}$) mouse, stained for DβH. (b) Quantitation of DβH staining shows no change in the HC due to BDNF depletion. (c) Quantitation of DβH staining in the CB of the same mice also shows no difference in DβH staining. Data show mean ± SEM, $n = 4$ matched pairs, 8 to 12 sections per region per animal. Results of student's paired t tests are nonsignificant. (d) Comparison of DβH staining in HC of WT to 5XFAD mice, $n = 3$ per group, 8 to 12 sections per region per mouse.
*$p < .05$, Student's paired t test.

innervation that occurs in aged animals. The precise causes of increased innervation are not known but may be due to the fact that the LC is highly plastic in response to injury (Fritschy and Grzanna, 1992), and plaque deposition itself can lead to increased or aberrant axonal sprouting (Phinney et al., 1999).

The 5XFAD:BDNF$^{f/f}$ mice also displayed decreased NAergic innervation in remote regions despite local depletion of HC BDNF. In the CTX, there was a non-significant reduction in DβH staining along with significant reductions in TH staining in the rostral LC, which should contain cells providing NAergic input to both the HC and CTX. These data are consistent with two mutually inclusive alternative possibilities: The first is that the HC projects to (Jay and Witter, 1991) and delivers BDNF to CTX, so depletion of HC BDNF results in reduced CTX BDNF. Alternatively, HC BDNF depletion may damage LC neurons that also innervate other regions due to extensive collateralization of LC neurons (Aghajanian et al., 1977; Foote and Morrison, 1987). In this way, targeted BDNF depletion in one area could broadly stress LC neurons throughout the nucleus. In an attempt to distinguish further between the two possibilities, the CB was included for analysis as a region that

should not be directly affected by hippocampal BDNF depletion. Interestingly, DβH staining was reduced in this area as well. Since the LC also innervates the CB, these data imply that remote changes in NAergic innervation are due to damage within the LC proper.

BDNF Depletion Damages the LC/NA System and Enhances AD-Type Pathology

We found that BDNF depletion from the HC led to a significant increase in amyloid plaque burden in the CTX, as compared with the control hemisphere. An increase in plaque burden is consistent with the effects of LC/NA depletion observed in other models, which has been attributed to increased inflammation of surrounding glial cells (Jardanhazi-Kurutz et al., 2011), altered amyloid processing (Jardanhazi-Kurutz et al., 2010), reduced levels of metalloproteinases responsible for Aβ degradation (Kalinin et al., 2007, 2012), and reduced microglial phagocytosis of Aβ plaques (Heneka et al., 2010). Whether some or all of these mechanisms account for our findings remains to be determined; however, our data indicate the latter effect may play a role. Significantly, we observed a decrease of Iba1 stained
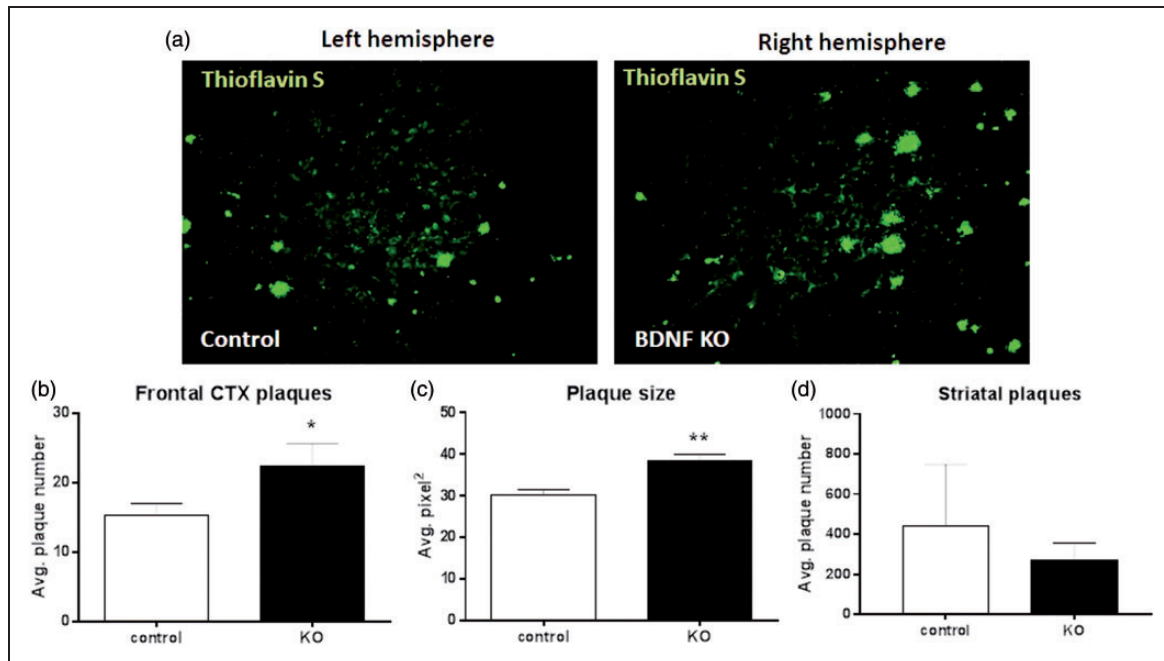
Figure 7. Hippocampus brain-derived neurotrophic factor depletion increases plaque load in cortex.
(a) Representative sagittal images from the contralateral (left, control) and ipsilateral (right, BDNF KO) frontal CTX relative to the site of BDNF depletion, stained for plaques using Thioflavin S. Quantitation shows that both (b) plaque number and (c) plaque size were significantly increased in the BDNF KO CTX. In contrast, BDNF depletion did not alter plaque load in the striatum (d). Data show mean $\pm$ SEM, $n = 4$ matched pairs, 8 to 12 sections per side per mouse.
$*p < .05$. $**p < .01$, Student's paired t test.

microglia in the same region where increased amyloid plaques were seen. The cause of the reduced Iba1 staining is not known; however, NA is known to enhance microglial migration to, and phagocytosis of, Aβ plaques (Heneka et al., 2010; Kalinin et al., 2012). The strong correlation between DβH staining and Iba1 staining supports the idea that NAergic innervation is also required for microglial survival or maintenance. However, it is also possible that hippocampal BDNF depletion directly influences microglial activation, since BDNF has been shown to cause an inflammatory response in microglia (Jiang et al., 2010). The decline in microglial activation may therefore also be due in part to decreased delivery of BDNF to the CTX from the HC. However, the finding that plaque pathology in the striatum, a region that accumulates plaques but does not receive much or any LC innervation (Rudelli et al., 1984; Ferrucci et al., 2013) was not influenced by BDNF depletion supports the notion that NAergic mechanisms play a role.

Our results show that loss of HC BDNF led to an increase in cortical amyloid plaque numbers. The consequences of BDNF deficiency on AD-type pathology have been reported earlier. In 5XFAD mice, hemizygous KO of TrkB worsened HC-dependent memory tasks (Devi and Ohno, 2015), while in APPswe/PS1dE9 transgenic mice (APdE9), overexpression of TrkB.T1, a truncated inactive form of TrkB, increased spatial memory impairment while the overexpression of TrkB.TK alleviated it (Kemppainen et al., 2012; Rantamaki et al., 2013). However, in contrast to our findings, in neither study did the authors observe differences in amyloid burden, Aβ concentrations, or amyloidogenic processing of amyloid precursor protein. A lack of effect of BDNF deficiency on amyloid burden (as well as tau pathology) was also observed in triple transgenic 3XTg-AD mice that had hemizygous KO of BDNF (Castello et al., 2012). The causes for this discrepancy are not clear; however, significant differences exist between the studies. In the TrkB (Devi and Ohno, 2015) and BDNF (Castello et al., 2012) KO studies, the gene KO was neither tissue nor cell specific, but was global, and was present from earliest development through adulthood, allowing for compensatory events to occur. In our study, BDNF depletion occurred only in the HC, and in adult mice therefore minimizing compensatory responses. In the TrkB KO study, the 5XFAD mice were examined at 4 to 5 months, a time there is significant, but not maximal amyloid deposition; in our study, mice were 7.0 to 7.5 months, a time at which amyloid deposition is significantly greater. We propose that lack of HC BDNF reduces BDNF signaling at TrkB receptors on LC
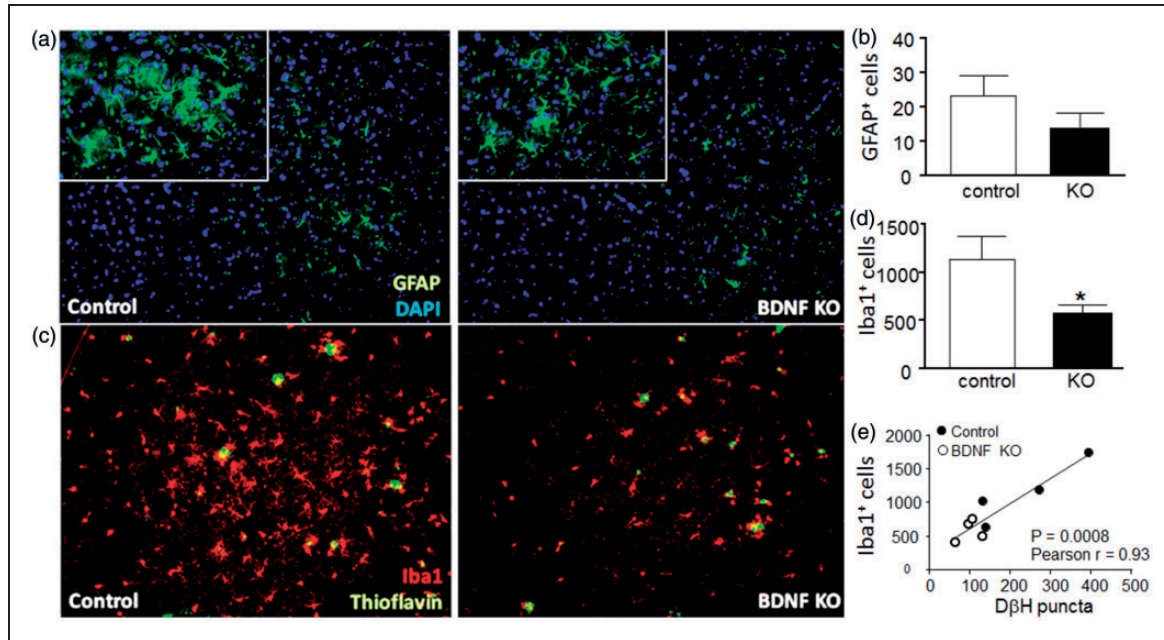
Figure 8. Hippocampus brain-derived neurotrophic factor depletion reduces microglial activation in cortex.
Representative sagittal images from the contralateral (left, control) and ipsilateral (right, BDNF KO) frontal CTX relative to the site of BDNF depletion, showing immunostaining for astrocyte marker GFAP (a) and microglial marker Iba1 (c). Quantitative analyses for number of GFAP (b) and Iba1 (d) positively stained cells show a decrease of Iba1 staining in the BDNF KO CTX. Data show mean $\pm$ SEM, $n = 4$ paired samples, 8 to 12 sections per side per mouse. $*p < .05$, Students paired t test. (e) The number of Iba1 + cells was compared with the number of DβH puncta counted in the same sections, from both the control (filled circles) and the BDNF KO (open circles) cortices. Correlation analysis of the entire data set revealed a significant positive correlation, Pearson's $r = 0.93$, $p = .0008$.
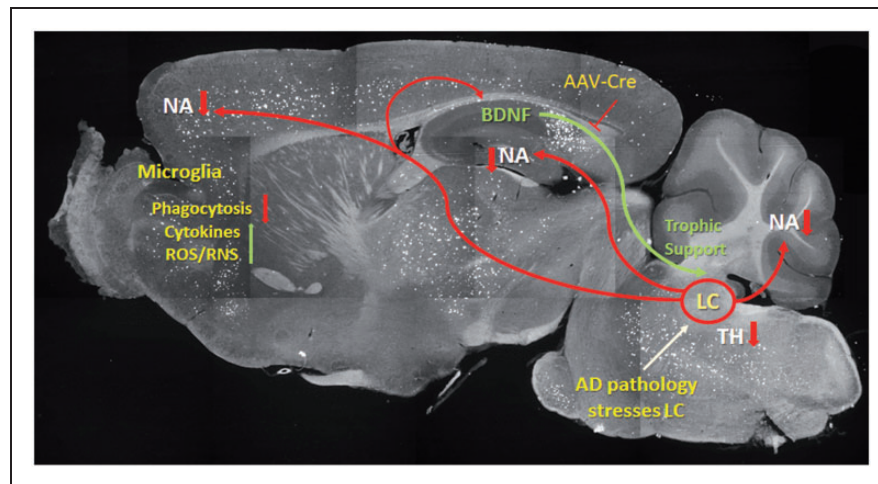
Figure 9. Schematic illustrating brain-derived neurotrophic factor depletion effects on Alzheimer's disease-type pathology.
The image shows a sagittal section from a 5XFAD mouse stained with thioflavin S to detect amyloid plaques. BDNF produced in the hippocampus is retrogradely transported to neuronal cell bodies in the locus coeruleus (LC) where it provides neurotrophic support. The LC normally provides NAergic innervation to all parts of the CNS, which regulates microglial functions, including phagocytosis, as well as production of pro-inflammatory factors. In the context of disease (in this case AD-type pathology), the LC neurons are damaged due to reductions in HC BDNF levels due to introduction of AAV-CMV-Cre into BDNF$^{f/f}$ mice, or to other genetic, environmental, or disease-related causes. This in turn decreases NAergic signaling, which reduces microglial (and astroglial) phagocytosis of amyloid.

neurons having terminals within the HC leading to LC damage, a possibility supported by our findings that ThioS staining was increased in the CTX but not in the striatum, a region which does not receive significant NAergic innervation. If so, it may be that in the other studies genetic depletion of BDNF or TrkB did not result in significant LC damage, dysfunction, or loss of NAergic signaling to the CTX. Similarly, in mice where TrkB.T1 was overexpressed, the promoter (Thy1) would be to direct expression to CTX and HC neurons but not to LC neurons which explain lack of LC damage.

The current experimental design was such that each animal served as its own control. Since LC projections to HC are both ipsilateral and contralateral, there are some effects of BDNF depletion on the contralateral hemisphere. The LC projections are primarily ipsilateral, however, and it has been estimated from tracer studies that only about 7% to 15% of projections to the HC are contralateral (Ader et al., 1980; Room et al., 1981). Furthermore, within the hippocampal formations, BDNF transport experiments have shown that little if any BDNF moves contralaterally across hemispheres (DiStefano et al., 1992). In any case, the effect of such contralateral actions would be to reduce the effect size observed between control and BDNF KO hemispheres. A second concern is that the AAV virus itself can be anterogradely or retrogradely transported (Castle et al., 2014). The majority of such transport would likely occur within the HC; however, virus could also move outside of this region. The fact that the GFP signal was largely undetected outside of the body of the HC suggests that viral transport and BDNF depletion outside of the HC was minimal.

The current study supports the idea that the LC/NA system is a viable target for ameliorating AD pathology, and that current efforts testing small-molecule modulators of BDNF receptors may be of value. There is substantial preclinical evidence that BDNF itself (Arancibia et al., 2008; Nagahara et al., 2009) or synthetic TrkB ligands provide therapeutic benefit in the AD context (Nagahara et al., 2009). The TrkB agonist 7,8-dihydroxyflavone (DHF), for example, provides substantial benefit in several mouse models of AD (Devi and Ohno, 2012; Castello et al., 2014; Zhang et al., 2014). Intraperitoneal injection of DHF once daily for 10 days in 12- to 15-month-old mice resulted in an increase in hippocampal TrkB phosphorylation, complete rescue of cognitive impairment in the spontaneous alternation Y-maze task, acutely decreased expression of beta-secretase, and reduced levels of $A\beta_{40}$ and $_{42}$. Although the effects of treatment with DHF on the LC were not examined, our results suggest that the benefits conferred by DHF treatment include preservation of LC function.

References

Ader, J. P., Room, P., Postema, F., & Korf, J. (1980). Bilaterally diverging axon collaterals and contralateral projections from rat locus coeruleus neurons, demonstrated by fluorescent retrograde double labeling and norepinephrine metabolism. *J Neural Transm*, *49*, 207–208.

Aghajanian, G. K., Cedarbaum, J. M., & Wang, R. Y. (1977). Evidence for norepinephrine-mediated collateral inhibition of locus coeruleus neurons. *Brain Res*, *136*, 570–577.

Ahmed, B. Y., Chakravarthy, S., Eggers, R., Hermens, W. T., Zhang, J. Y., Niclou, S. P., Levelt, C., Sablitzky, F., Anderson, P. N., Lieberman, A. R., & Verhaagen, J. (2004). Efficient delivery of cre-recombinase to neurons in vivo and stable transduction of neurons using adeno-associated and lentiviral vectors. *BMC Neurosci*, *5*, 4.

Arancibia, S., Silhol, M., Mouliere, F., Meffre, J., Hollinger, I., Maurice, T., & Tapia-Arancibia, L. (2008). Protective effect of BDNF against beta-amyloid induced neurotoxicity in vitro and in vivo in rats. *Neurobiol Dis*, *31*, 316–326.

Aschauer, D. F., Kreuz, S., & Rumpel, S. (2013). Analysis of transduction efficiency, tropism and axonal transport of AAV serotypes, 1, 2, 5, 6, 8 and 9 in the mouse brain. *PLoS One*, *8*, e76310.

Braun, D., Madrigal, J. L., & Feinstein, D. L. (2014). Noradrenergic regulation of glial activation: Molecular mechanisms and therapeutic implications. *Curr Neuropharmacol*, *12*, 342–352.

Castello, N. A., Green, K. N., & LaFerla, F. M. (2012). Genetic knockdown of brain-derived neurotrophic factor in 3xTg-AD mice does not alter Abeta or tau pathology. *PLoS One*, *7*, e39566.

Castello, N. A., Nguyen, M. H., Tran, J. D., Cheng, D., Green, K. N., & LaFerla, F. M. (2014). 7,8-Dihydroxyflavone, a small molecule TrkB agonist, improves spatial memory and increases thin spine density in a mouse model of Alzheimer disease-like neuronal loss. *PLoS One*, *9*, e91453.

Castle, M. J., Perlson, E., Holzbaur, E. L., & Wolfe, J. H. (2014). Long-distance axonal transport of AAV9 is driven by dynein and kinesin-2 and is trafficked in a highly motile Rab7-positive compartment. *Mol Ther*, *22*, 554–566.

Chen, M. J., Nguyen, T. V., Pike, C. J., & Russo-Neustadt, A. A. (2007). Norepinephrine induces BDNF and activates the PI-3K

and MAPK cascades in embryonic hippocampal neurons. *Cell Signal*, 19, 114–128.

Chris, Z., Scott, A. L., James, A. M., & Helena, C. C. (2003). Neuronal loss is greater in the locus coeruleus than nucleus basalis and substantia nigra in Alzheimer and Parkinson diseases. *Arch Neurol*, 60, 337–341.

Combarros, O., Warden, D. R., Hammond, N., Cortina-Borja, M., Belbin, O., Lehmann, M. G., Wilcock, G. K., Brown, K., Kehoe, P. G., Barber, R., Coto, E., Alvarez, V., Deloukas, P., Gwilliam, R., Heun, R., Kölsch, H., Mateo, I., Oulhaj, A., Arias-Vásquez, A., Schuur, M., Aulchenko, Y. S., Ikram, M. A., Breteler, M. M., van Duijn, C. M., Morgan, K., Smith, A. D., & Lehmann, D. J. (2010). The dopamine beta-hydroxylase-1021C/T polymorphism is associated with the risk of Alzheimer's disease in the Epistasis Project. *BMC Med Genet*, 11, 162.

Connor, B., Young, D., Yan, Q., Faull, R. L. M., Synek, B., & Dragunow, M. (1997). Brain-derived neurotrophic factor is reduced in Alzheimer's disease. *Mol Brain Res*, 49, 71–81.

Devi, L., & Ohno, M. (2012). 7,8-dihydroxyflavone, a small-molecule TrkB agonist, reverses memory deficits and BACE1 elevation in a mouse model of Alzheimer's disease. *Neuropsychopharmacology*, 37, 434–444.

Devi, L., & Ohno, M. (2015). TrkB reduction exacerbates Alzheimer's disease-like signaling aberrations and memory deficits without affecting beta-amyloidosis in 5XFAD mice. *Transl Psychiatry*, 5, e562.

DiStefano, P. S., Friedman, B., Radziejewski, C., Alexander, C., Boland, P., Schick, C. M., Lindsay, R. M., & Wiegand, S. J. (1992). The neurotrophins BDNF, NT-3, and NGF display distinct patterns of retrograde axonal transport in peripheral and central neurons. *Neuron*, 8, 983–993.

Ferrucci, M., Giorgi, F. S., Bartalucci, A., Busceti, C. L., & Fornai, F. (2013). The effects of locus coeruleus and norepinephrine in methamphetamine toxicity. *Curr Neuropharmacol*, 11, 80–94.

Foote, S. L., & Morrison, J. H. (1987). Extrathalamic modulation of cortical function. *Ann Rev Neurosci*, 10, 67–95.

Fritschy, J. M., & Grzanna, R. (1992). Restoration of ascending noradrenergic projections by residual locus coeruleus neurons: Compensatory response to neurotoxin-induced cell death in the adult rat brain. *J Comp Neurol*, 321, 421–441.

German, D. C., Nelson, O., Liang, F., Liang, C. L., & Games, D. (2005). The PDAPP mouse model of Alzheimer's disease: Locus coeruleus neuronal shrinkage. *J Comp Neurol*, 492, 469–476.

Guo, M., Huang, T. Y., Garza, J. C., Chua, S. C., & Lu, X. Y. (2013). Selective deletion of leptin receptors in adult hippocampus induces depression-related behaviours. *Int J Neuropsychopharmacol*, 16, 857–867.

Heldt, S. A., Stanek, L., Chhatwal, J. P., & Ressler, K. J. (2007). Hippocampus-specific deletion of BDNF in adult mice impairs spatial memory and extinction of aversive memories. *Mol Psychiatry*, 12, 656–670.

Heneka, M. T., Nadrigny, F., Regen, T., Martinez-Hernandez, A., Dumitrescu-Ozimek, L., Terwel, D., Jardanhazi-Kurutz, D., Walter, J., Kirchhoff, F., Hanisch, U.-. K. K., & Kummer, M. P. (2010). Locus ceruleus controls Alzheimer's disease pathology by modulating microglial functions through norepinephrine. *Proc Natl Acad Sci USA*, 107, 6058–6063.

Holm, P. C., Rodríguez, F. J., Kresse, A., Canals, J. M., Silos-Santiago, I., & Arenas, E. (2003). Crucial role of TrkB ligands in the survival and phenotypic differentiation of developing locus coeruleus noradrenergic neurons. *Development*, 130, 3535–3545.

Hopp, S. C., Royer, S. E., D'Angelo, H. M., Kaercher, R. M., Fisher, D. A., & Wenk, G. L. (2015). Differential neuroprotective and anti-inflammatory effects of L-type voltage dependent calcium channel and ryanodine receptor antagonists in the substantia nigra and locus coeruleus. *J Neuroimmune Pharmacol*, 10, 35–44.

Jardanhazi-Kurutz, D., Kummer, M. P., Terwel, D., Vogel, K., Dyrks, T., Thiele, A., & Heneka, M. T. (2010). Induced LC degeneration in APP/PS1 transgenic mice accelerates early cerebral amyloidosis and cognitive deficits. Induced LC degeneration in APP/PS1 transgenic mice accelerates early cerebral amyloidosis and cognitive deficits. *Neurochem Int*, 57, 375–382.

Jardanhazi-Kurutz, D., Kummer, M. P., Terwel, D., Vogel, K., Thiele, A., & Heneka, M. T. (2011). Distinct adrenergic system changes and neuroinflammation in response to induced locus ceruleus degeneration in APP/PS1 transgenic mice. Distinct adrenergic system changes and neuroinflammation in response to induced locus ceruleus degeneration in APP/PS1 transgenic mice. *Neuroscience*, 176, 396–407.

Jay, T. M., & Witter, M. P. (1991). Distribution of hippocampal CA1 and subicular efferents in the prefrontal cortex of the rat studied by means of anterograde transport of Phaseolus vulgaris leucoagglutinin. *J Comp Neurol*, 313, 574–586.

Jiang, Y., Wei, N., Zhu, J., Lu, T., Chen, Z., Xu, G., & Liu, X. (2010). Effects of brain-derived neurotrophic factor on local inflammation in experimental stroke of rat. *Mediators Inflamm*, 2010, 372–423.

Jurič, D., Lončar, D., & Čarman-Kržan, M. (2008). Noradrenergic stimulation of BDNF synthesis in astrocytes: Mediation via α1- and β1/β2-adrenergic receptors. *Neurochem Int*, 52, 297–306.

Kalinin, S., Gavrilyuk, V., Polak, P. E., Vasser, R., Zhao, J., Heneka, M. T., & Feinstein, D. L. (2007). Noradrenaline deficiency in brain increases β-amyloid plaque burden in an animal model of Alzheimer's disease. *Neurobiol Aging*, 28, 1206–1214.

Kalinin, S., Polak, P. E., Lin, S., Sakharkar, A. J., Pandey, S. C., & Feinstein, D. L. (2012). The noradrenaline precursor L-DOPS reduces pathology in a mouse model of Alzheimer's disease. *Neurobiol Aging*, 33, 1651–1663.

Kaneko, Y. S., Mori, K., Nakashima, A., Sawada, M., Nagatsu, I., & Ota, A. (2005). Peripheral injection of lipopolysaccharide enhances expression of inflammatory cytokines in murine locus coeruleus: Possible role of increased norepinephrine turnover. *J Neurochem*, 94, 393–404.

Karra, D., & Dahm, R. (2010). Transfection techniques for neuronal cells. *J Neurosci*, 30, 6171–6177.

Kaspar, B. K., Vissel, B., Bengoechea, T., Crone, S., Randolph-Moore, L., Muller, R., Brandon, E. P., Schaffer, D., Verma, I. M., Lee, K. F., Heinemann, S. F., & Gage, F. H. (2002). Adeno-associated virus effectively mediates conditional gene modification in the brain. *Proc Natl Acad Sci USA*, 99, 2320–2325.

Kemppainen, S., Rantamaki, T., Jeronimo-Santos, A., Lavasseur, G., Autio, H., Karpova, N., Karkkainen, E., Staven, S., Vicente

Miranda, H., Outeiro, T. F., Diogenes, M. J., Laroche, S., Davis, S., Sebastiao, A. M., Castren, E., & Tanila, H. (2012). Impaired TrkB receptor signaling contributes to memory impairment in APP/PS1 mice. *Neurobiol Aging*, *33*, 1122.e1123–1139.

Luellen, B. A., Bianco, L. E., Schneider, L. M., & Andrews, A. M. (2007). Reduced brain derived neurotrophic factor is associated with a loss of serotonergic innervation in the hippocampus of aging mice. *Genes Brain Behav*, *6*, 482–490.

Manaye, K. F., McIntire, D. D., Mann, D. M. A., & German, D. C. (1995). Locus coeruleus cell loss in the aging human brain: A non random process. *J Comp Neurol*, *358*, 79–87.

Mann, D. M. (1983). The locus coeruleus and its possible role in ageing and degenerative disease of the human central nervous system. *Mech Ageing Dev*, *23*, 73–94.

Marcyniuk, B., Mann, D. M., & Yates, P. O. (1986). The topography of cell loss from locus caeruleus in Alzheimer's disease. *J Neurol Sci*, *76*, 335–345.

Matsunaga, W., Isobe, K., & Shirokawa, T. (2006). Involvement of neurotrophic factors in aging of noradrenergic innervations in hippocampus and frontal cortex. *Neurosci Res*, *54*, 313–318.

Matsunaga, W., Shirokawa, T., & Isobe, K. (2004). BDNF is necessary for maintenance of noradrenergic innervations in the aged rat brain. *Neurobiol Aging*, *25*, 341–348.

Nagahara, A. H., Merrill, D. A., Coppola, G., Tsukada, S., Schroeder, B. E., Shaked, G. M., Wang, L., Blesch, A., Kim, A., Conner, J. M., Rockenstein, E., Chao, M. V., Koo, E. H., Geschwind, D., Masliah, E., Chiba, A. A., & Tuszynski, M. H. (2009). Neuroprotective effects of brain-derived neurotrophic factor in rodent and primate models of Alzheimer's disease. *Nat Med*, *15*, 331–337.

Nakai, S., Matsunaga, W., Ishida, Y., Isobe, K.- I., & Shirokawa, T. (2006). Effects of BDNF infusion on the axon terminals of locus coeruleus neurons of aging rats. *Neurosci Res*, *54*, 213–219.

Ohno, M., Sametsky, E. A., Younkin, L. H., Oakley, H., Younkin, S. G., Citron, M., Vassar, R., & Disterhoft, J. F. (2004). BACE1 deficiency rescues memory deficits and cholinergic dysfunction in a mouse model of Alzheimer's disease. *Neuron*, *41*, 27–33.

Onksen, J. L., Briand, L. A., Galante, R. J., Pack, A. I., & Blendy, J. A. (2012). Running-induced anxiety is dependent on increases in hippocampal neurogenesis. *Genes Brain Behav*, *11*, 529–538.

Pamphlett, R. (2014). Uptake of environmental toxicants by the locus ceruleus: A potential trigger for neurodegenerative, demyelinating and psychiatric disorders. *Med Hypotheses*, *82*, 97–104.

Peskind, E. R., Tsuang, D. W., Bonner, L. T., Pascualy, M., Riekse, R. G., Snowden, M. B., Thomas, R., & Raskind, M. A. (2005). Propranolol for disruptive behaviors in nursing home residents with probable or possible Alzheimer disease: A placebo-controlled study. *Alzheimer Dis Assoc Disord*, *19*, 23–28.

Phinney, A. L., Deller, T., Stalder, M., Calhoun, M. E., Frotscher, M., Sommer, B., Staufenbiel, M., & Jucker, M. (1999). Cerebral amyloid induces aberrant axonal sprouting and ectopic terminal formation in amyloid precursor protein transgenic mice. *J Neurosci*, *19*, 8552–8559.

Rantamaki, T., Kemppainen, S., Autio, H., Staven, S., Koivisto, H., Kojima, M., Antila, H., Miettinen, P. O., Karkkainen, E., Karpova, N., Vesa, L., Lindemann, L., Hoener, M. C., Tanila, H., & Castren, E. (2013). The impact of Bdnf gene deficiency to the memory impairment and brain pathology of APPswe/ PS1dE9 mouse model of Alzheimer's disease. *PLoS One*, *8*, e68722.

Raskind, M. A., Peskind, E. R., Holmes, C., & Goldstein, D. S. (1999). Patterns of cerebrospinal fluid catechols support increased central noradrenergic responsiveness in aging and Alzheimer's disease. *Biol Psychiatry*, *46*, 756–765.

Rios, M., Fan, G., Fekete, C., Kelly, J., Bates, B., Kuehn, R., Lechan, R. M., & Jaenisch, R. (2001). Conditional deletion of brain-derived neurotrophic factor in the postnatal brain leads to obesity and hyperactivity. *Mol Endocrinol*, *15*, 1748–1757.

Room, P., Postema, F., & Korf, J. (1981). Divergent axon collaterals of rat locus coeruleus neurons: Demonstration by a fluorescent double labeling technique. *Brain Res*, *221*, 219–230.

Rudelli, R. D., Ambler, M. W., & Wisniewski, H. M. (1984). Morphology and distribution of Alzheimer neuritic (senile) and amyloid plaques in striatum and diencephalon. *Acta Neuropathol*, *64*, 273–281.

Sabine, T., Marc, M., Elodie, M., Etienne, C. H., & Patrick, P. M. (2006). The phenotypic differentiation of locus ceruleus noradrenergic neurons mediated by brain-derived neurotrophic factor is enhanced by corticotropin releasing factor through the activation of a camp-dependent signaling pathway. *Mol Pharmacol*, *70*, 30–40.

Sanchez-Padilla, J., Guzman, J. N., Ilijic, E., Kondapalli, J., Galtieri, D. J., Yang, B., Schieber, S., Oertel, W., Wokosin, D., Schumacker, P. T., & Surmeier, J. D. (2014). Mitochondrial oxidant stress in locus coeruleus is regulated by activity and nitric oxide synthase. *Nat Neurosci*, *17*, 832–840.

Szabadi, E. (2013). Functional neuroanatomy of the central noradrenergic system. *J Psychopharmacol*, *27*, 659–693.

Tekin, I., Roskoski, R., Carkaci-Salli, N., & Vrana, K. E. (2014). Complex molecular regulation of tyrosine hydroxylase. *J Neural Transm*, *121*, 1451–1481.

Trojanowski, J. Q., Atkinson, B., & Lee, V. M. (1986). An immunocytochemical study of normal and abnormal human cerebrospinal fluid with monoclonal antibodies to glial fibrillary acidic protein. *Acta Cytol*, *30*, 235–239.

Wang, L. Y., Shofer, J. B., Rohde, K., Hart, K. L., Hoff, D. J., McFall, Y. H., Raskind, M. A., & Peskind, E. R. (2009). Prazosin for the treatment of behavioral symptoms in patients with alzheimer disease with agitation and aggression. *Am J Geriatr Psychiatry*, *17*, 744–751.

Wei, C. J., Augusto, E., Gomes, C. A., Singer, P., Wang, Y., Boison, D., Cunha, R. A., Yee, B. K., & Chen, J. F. (2014). Regulation of fear responses by striatal and extrastriatal adenosine A2A receptors in forebrain. *Biol Psychiatry*, *75*, 855–863.

Yang, P., Qin, Y., Zhang, W., Bian, Z., & Wang, R. (2015). Sensorimotor cortex injection of adeno-associated viral vector mediates knockout of PTEN in neurons of the brain and spinal cord of mice. *J Mol Neurosci*, *57*, 470–476.

Yu, J.-T., Tan, L., Ou, J.-R., Zhu, J.-X., Liu, K., Song, J.-H., & Sun, Y. -P. (2008). Polymorphisms at the β2-adrenergic receptor gene influence Alzheimer's disease susceptibility. *Brain Res*, *1210*, 216–222.

Zhang, Z., Liu, X., Schroeder, J. P., Chan, C. B., Song, M., Yu, S. P., Weinshenker, D., & Ye, K. (2014). 7,8-dihydroxyflavone prevents synaptic loss and memory deficits in a mouse model of Alzheimer's disease. *Neuropsychopharmacology*, *39*, 638–650.